nature climate change

LETTERS

PUBLISHED ONLINE: 19 JANUARY 2014 | DOI: 10.1038/NCLIMATE2100

Increasing frequency of extreme El Niño events due to greenhouse warming

Wenju Cai[1,2]*, Simon Borlace[1], Matthieu Lengaigne[3], Peter van Rensch[1], Mat Collins[4], Gabriel Vecchi[5], Axel Timmermann[6], Agus Santoso[7], Michael J. McPhaden[8], Lixin Wu[2], Matthew H. England[7], Guojian Wang[1,2], Eric Guilyardi[3,9] and Fei-Fei Jin[10]

El Niño events are a prominent feature of climate variability with global climatic impacts. The 1997/98 episode, often referred to as 'the climate event of the twentieth century'[1,2], and the 1982/83 extreme El Niño[3], featured a pronounced eastward extension of the west Pacific warm pool and development of atmospheric convection, and hence a huge rainfall increase, in the usually cold and dry equatorial eastern Pacific. Such a massive reorganization of atmospheric convection, which we define as an extreme El Niño, severely disrupted global weather patterns, affecting ecosystems[4,5], agriculture[6], tropical cyclones, drought, bushfires, floods and other extreme weather events worldwide[3,7–9]. Potential future changes in such extreme El Niño occurrences could have profound socio-economic consequences. Here we present climate modelling evidence for a doubling in the occurrences in the future in response to greenhouse warming. We estimate the change by aggregating results from climate models in the Coupled Model Intercomparison Project phases 3 (CMIP3; ref. 10) and 5 (CMIP5; ref. 11) multi-model databases, and a perturbed physics ensemble[12]. The increased frequency arises from a projected surface warming over the eastern equatorial Pacific that occurs faster than in the surrounding ocean waters[13,14], facilitating more occurrences of atmospheric convection in the eastern equatorial region.

The 1982/83 and 1997/98 extreme El Niño events were characterized by an exceptional warming, with sea surface temperatures (SSTs) exceeding 28 °C extending into the eastern equatorial Pacific[2,3]. This led to an equatorward shift of the intertropical convergence zone (ITCZ), and hence intense rainfall in the equatorial eastern Pacific where cold and dry conditions normally prevail. This major reorganization of atmospheric convection severely disrupted global weather patterns and spurred major natural disasters. Catastrophic floods occurred in the eastern equatorial region of Ecuador and northern Peru[3,7], and neighbouring regions to the south and north experienced severe droughts (Supplementary Fig. 1). The anomalous conditions caused widespread environmental disruptions, including the disappearance of marine life and decimation of the native bird population in the Galapagos Islands[15,16], and severe bleaching of corals in the Pacific and beyond[4,5]. The impacts extended to every continent, and the 1997/98 event alone caused US$35–45 billion in damage and claimed an estimated 23,000 human lives worldwide[17].

The devastating impacts demand an examination of whether greenhouse warming will alter the frequency of such extreme El Niño events. Although many studies have examined the effects of a projected warming on the Pacific mean state, El Niño diversity and El Niño teleconnections[18–21], the issue of how extreme El Niños will change has not been investigated. Here we show that greenhouse warming leads to a significant increase in the frequency of such events.

We contrast the characteristics between the extreme and moderate El Niño events using available data sets[22,23], focusing on December–January–February (DJF), the season in which El Niño events peak. During moderate events, which include canonical and Modoki El Niño[24], the eastern boundary of the warm pool (indicated by the 28 °C isotherm, purple, Fig. 1a) and the atmospheric convective zone move eastwards to just east of the Date Line. The ITCZ lies north of the Equator[25], and the rainfall anomaly over the eastern equatorial Pacific is small (Fig. 1a).

During extreme El Niño, the warm pool expands eastward and eventually covers the entire equatorial Pacific (Fig. 1b), markedly weakening the equatorial east–west and meridional SST gradients (Fig. 1c,d); the latter being defined as the difference between the northern off-equatorial (8° N, the ITCZ position) and the equatorial Pacific. Consequently convection, which follows the highest SSTs, extends eastward and the ITCZ shifts equatorward[25], leading to atmospheric convection and extraordinary rainfall (>5 mm per day, green, Fig. 1b) in the normally dry eastern equatorial Pacific. There, easterly winds are replaced by westerlies, which suppress the eastern equatorial upwelling[2,3], reinforcing the exceptionally high SSTs in this region. In association, Niño3 area-averaged rainfall increases nonlinearly with Niño3 SST (Fig. 1c) and the meridional SST gradient (Fig. 1d).

This striking rainfall nonlinearity is the distinct feature of an extreme El Niño, reflecting the pronounced shift in convective zone, with concurrent weakening of SST gradients in the eastern equatorial Pacific (Supplementary Fig. 3). Niño3 rainfall is thus a

[1]CSIRO Marine and Atmospheric Research, Aspendale, Victoria 3195, Australia, [2]Physical Oceanography Laboratory, Qingdao Collaborative Innovation Center of Marine Science and Technology, Ocean University of China, Qingdao 266003, China, [3]Laboratoire d'Océanographie et du Climat: Expérimentation et Approches Numériques (LOCEAN), IRD/UPMC/CNRS/MNHN, 75252 Paris Cedex 05, France, [4]College of Engineering Mathematics and Physical Sciences, Harrison Building, Streatham Campus, University of Exeter, Exeter EX1 3PB, UK, [5]Geophysical Fluid Dynamics Laboratory/NOAA, Princeton, New Jersey 08540-6649, USA, [6]IPRC, Department of Oceanography, SOEST, University of Hawaii, Honolulu, Hawaii 96822, USA, [7]Australian Research Council (ARC) Centre of Excellence for Climate System Science, Level 4 Mathews Building, The University of New South Wales, Sydney 2052, Australia, [8]NOAA/Pacific Marine Environmental Laboratory, Seattle, Washington 98115, USA, [9]NCAS-Climate, University of Reading, Reading RG6 6BB, UK, [10]Department of Meteorology, SOEST, University of Hawaii, Honolulu, Hawaii 96822, USA. *e-mail: Wenju.Cai@csiro.au

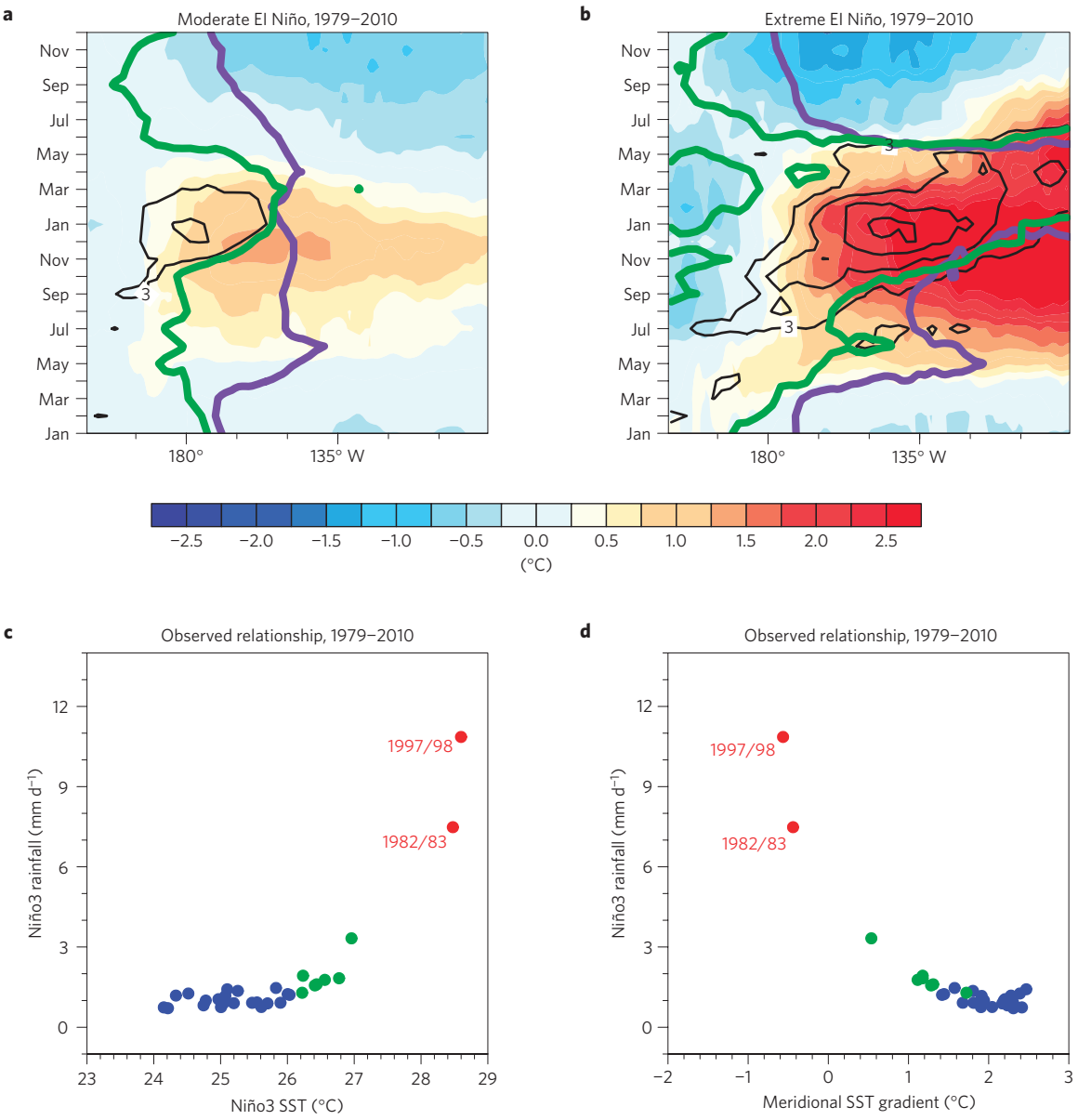

Figure 1 | Evolution and nonlinear characteristics of observed extreme El Niño events. a,**b**, Time–longitude diagram for composite moderate and extreme El Niño events, respectively, of equatorial SST anomalies (colour scale) and rainfall anomalies (contour, at intervals of 3 mm per day), 28 °C isotherm (purple curve) and total rainfall 5 mm per day isopleth (green curve). **c**,**d**, Relationship of eastern equatorial Pacific (Niño3 area: 5° S–5° N, 150° W–90° W) DJF total rainfall with DJF Niño3 SST and meridional SST gradients in the Niño3 longitude range. The meridional SST gradient is defined as the average SST over the off-equatorial region (5° N–10° N, 150° W–90° W) minus the average over the equatorial region (2.5° S–2.5° N, 150° W–90° W). Extreme El Niño (defined as events for which austral summer rainfall is greater than 5 mm per day), moderate El Niño (defined as events with SST anomalies greater than 0.5 s.d. of that over the period since 1979 that are not extreme El Niño events), and La Niña and neutral events, are indicated by red, green and blue dots respectively. During extreme El Niño, the meridional SST gradient diminishes, or reverses, shifting the ITCZ to the eastern equatorial Pacific.

good indicator of extreme El Niño[25,26], particularly because it is the anomalous convection and rainfall that in turn influence global weather. Rainfall is also an excellent measure for condensational heating of the atmosphere, thus providing an effective metric for large-scale atmospheric circulation anomalies. The observed rainfall nonlinearity can be measured by its skewness, which is greater than one over the period since 1979. We define an extreme El Niño as an event during which such massive reorganization of atmospheric convection takes place, leading to Niño3 rainfall that exceeds 5 mm per day; similar to a previous definition that used a rainfall anomaly threshold in the eastern Pacific[25]. Our definition distinctly identifies the 1982/83 and 1997/98 events as extreme El Niños.

The extraordinary large-scale changes over the tropical Pacific during an extreme El Niño mean that such events can induce extreme swings of the South Pacific convergence zone (SPCZ) (referred to as zonal SPCZ events), as occurred in 1982/83 and 1997/98 (refs 8,9). However, zonal SPCZ events can also occur without extreme El Niños[8], as in 1991/92. During the 1991/92 event, observations and reanalyses[23,24] show that the 28 °C isotherm, the 5 mm per day rainfall isopleths, or ascending motion, did not cover the entire Niño3 region, and the ITCZ was still situated north of the Equator (Supplementary Fig. 4), in stark contrast to the 1982/83 and 1997/98 extreme El Niño events (Supplementary Fig. 2c). As zonal SPCZ events can occur without extreme El Niños, as is also the case in the climate models considered here (Supplementary Fig. 5),

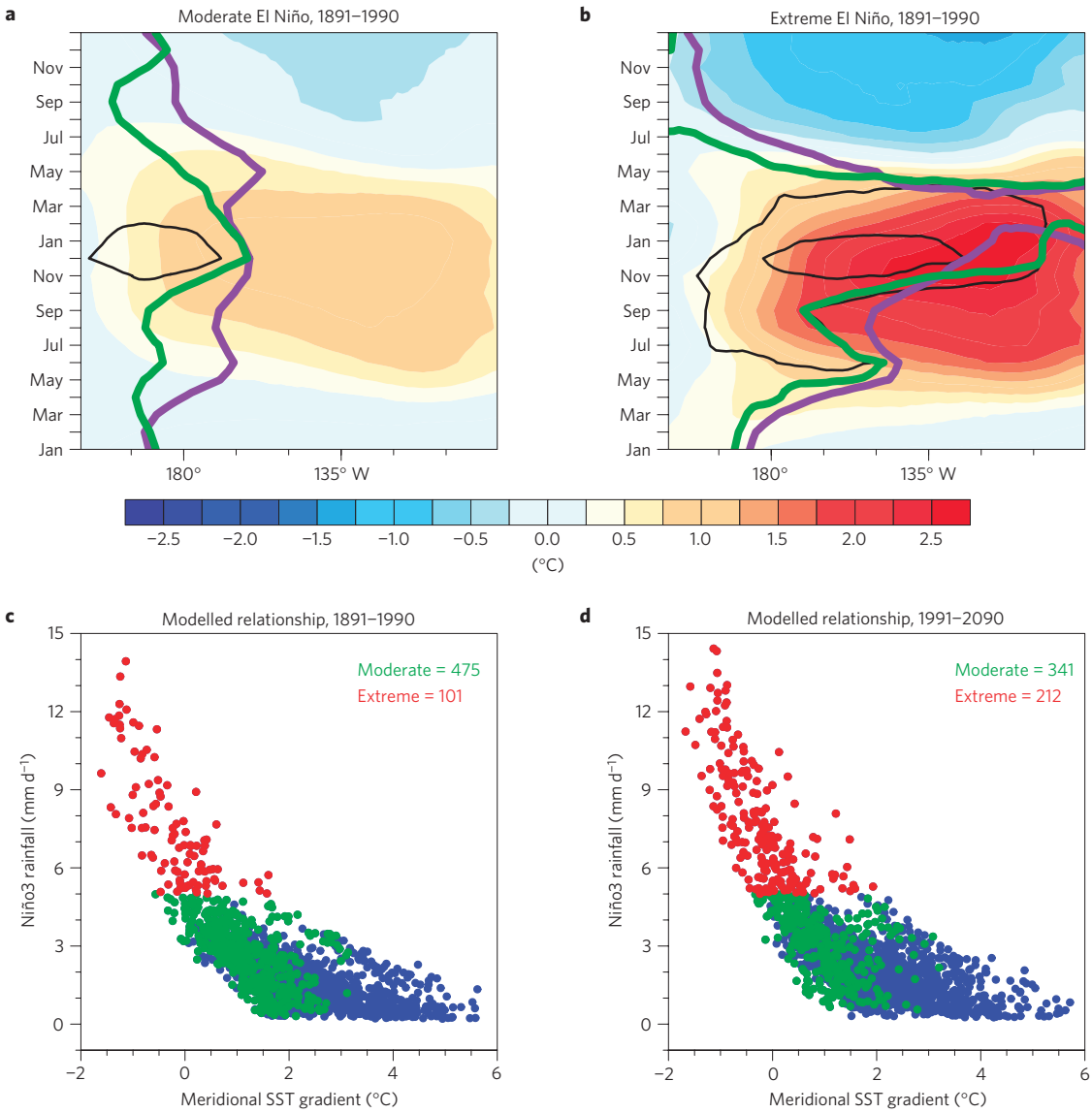

Figure 2 | Evolution and nonlinear characteristics of model extreme El Niño events, and changes in occurrences under greenhouse warming. **a**,**b**, Time–longitude diagram for composite moderate and extreme El Niño events, respectively, of equatorial SST anomalies (colour scale) and rainfall anomalies (contour, at intervals of 3 mm per day), 28 °C isotherm (purple curve) and total rainfall 5 mm per day isopleth (green curve) for the control period, illustrating simulation of the observed evolution. **c**,**d**, Relationship between eastern equatorial Pacific (Niño3 area: 5° S–5° N, 150° W–90° W) austral summer total rainfall and austral summer meridional SST gradient for the control and climate change periods, respectively. Red, green and blue dots indicate extreme El Niño (defined as events for which austral summer rainfall is greater than 5 mm per day), moderate El Niño (defined as events with SST anomalies greater than 0.5 s.d. of the control period that are not extreme El Niño events), and La Niña and neutral events, that is, all non-El Niño years, respectively. The number of moderate El Niño and extreme El Niño events in each period is shown.

increased occurrences of zonal SPCZ events under global warming[9] should not be used to infer a change in frequency of extreme El Niño events, an issue that is specifically examined here.

Not all coupled general circulation models (CGCMs) simulate the observed level of rainfall skewness. The CGCMs are forced with historical anthropogenic and natural forcings, and future greenhouse gas emission scenarios (Methods), each covering a 200-year period. We determine Niño3 rainfall skewness over the 200-year period in each model. Using skewness greater than 1 and Niño3 rainfall exceeding 5 mm per day as criteria for model selection, we identify 9 CMIP3 and 11 CMIP5 CGCMs that can simulate an extreme El Niño (Supplementary Figs 6–13 and Tables 1–2). For each of these 20 CGCMs, we compare the frequency of extreme El Niño in the first (1891–1990) and second (1991–2090) 100-year periods, referred to as the control and climate change periods, respectively.

The models reproduce the contrasts between moderate and extreme El Niño events (Fig. 2a,b) as seen in observations (Fig. 1a,b and Supplementary Fig. 2), associated with large reductions in meridional and zonal SST gradients (Supplementary Fig. 14). In aggregation, the total number of El Niño events decreases slightly but the total number of extreme El Niño events increases (Fig. 2c,d). The frequency of extreme El Niños doubles from about one event every 20 years (101 events in 2,000 years) in the control, to one every 10 years (212 events in 2,000 years) in the climate change period (Fig. 2c,d). This is statistically significant according to a bootstrap test[27], underscored by a strong inter-model consensus, with 17 out of 20 models simulating an increase (Supplementary Tables 1–2). These robust statistics are particularly compelling given the large inter-model differences in convective parameterizations[28]. Sensitivity tests to varying definitions of extreme El Niño (for

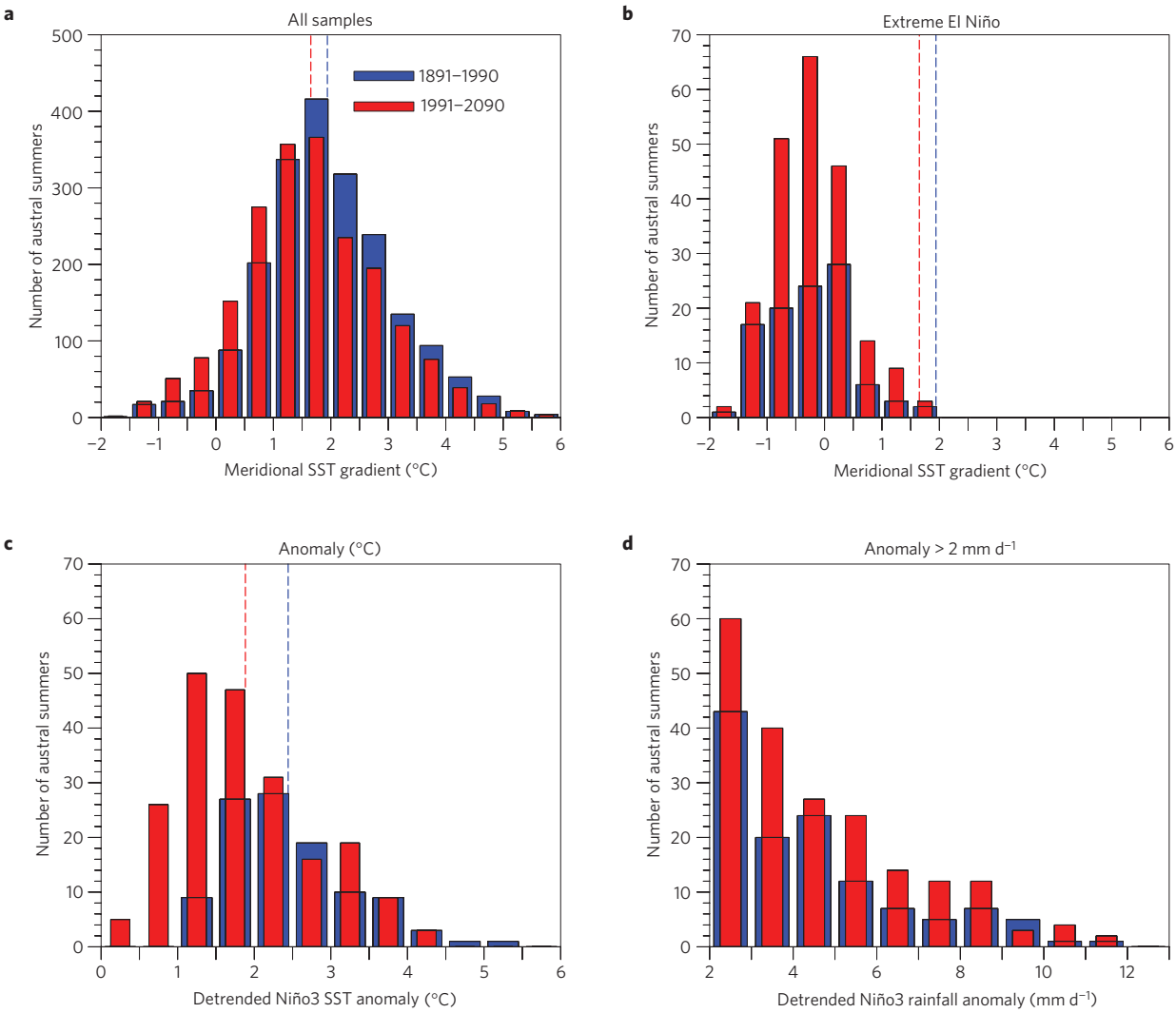

Figure 3 | Multi-model statistics associated with the increase in the frequency of extreme El Niño events. a,**b**, Multi-model histograms of the meridional SST gradient in the eastern equatorial Pacific for all samples, and for extreme El Niño alone. The meridional SST gradient is defined as the average SST over the east off-equatorial region (5° N–10° N, 150° E–90° W) minus the average over the eastern equatorial region (2.5° S–2.5° N, 155° E–120° W). All 2,000 samples in each period are distributed into 0.5 °C bins, for the control (blue) and climate change (red) periods. The multi-model climatological values for the control (blue dashed line) and the climate change (red dashed line) periods are indicated. **c**, Multi-model histogram of quadratically detrended SST anomalies for extreme El Niño events alone. **d**, Multi-model histogram of quadratically detrended rainfall anomalies for El Niño defined as Niño3 rainfall anomalies greater than 2 mm per day, showing changes in occurrences from control to the climate change period for given positive anomalies greater than 2 mm per day.

example, in conjunction with a diminishing meridional SST gradient, or using Niño3 rainfall relative to the western Pacific rainfall), or inclusion of all CGCMs, further support the robustness of this result (Supplementary Tables 3–6).

We assess the potential impact of the well-known cold SST bias using the HadCM3 CGCM, in which biases are corrected through a flux adjustment[12] in perturbed physics ensemble (PPE) experiments that produce extreme El Niño events. There is a fourfold increase in the frequency from one event in 60 years in the control to one event in 15 years in the climate change period (Supplementary Fig. 15 and Table 7). Thus, our conclusion remains valid in the absence of the SST biases. Although flux adjustments are not sufficient to correct all errors in models, this result does provide further evidence for future increase in extreme El Niño frequency.

The more frequent establishment of atmospheric convection in the eastern equatorial Pacific is induced by diminishing, or reversing, meridional and zonal SST gradients (Supplementary Fig. 14), rather than by a localized warming that exceeds the convective threshold range of the control period. For the latter to be true, the tropical convective area in recent decades and future climate simulations must expand, but there is no systematic evidence for this. Further, the CGCMs that are not selected, mostly with SSTs below the convective threshold in the control period, are unable to produce extreme El Niño events after the threshold is reached in the climate change period (Supplementary Figs 12–13), supporting the idea that convective threshold increases with mean SSTs (ref. 29).

The weakening of the SST gradients is induced by faster warming in the background state along the equatorial than in the off-equatorial Pacific, and in the eastern equatorial Pacific than in the west (Supplementary Fig. 16a)[13,14], a feature produced even without a dynamical ocean[30]. These slight changes in climatological SST gradient translate into a large increase in the occurrences of a diminished or reversed meridional SST gradient (Fig. 3a). This is associated with more occurrences of maximum SSTs, and hence convection, in the eastern equatorial Pacific for a given SST anomaly,

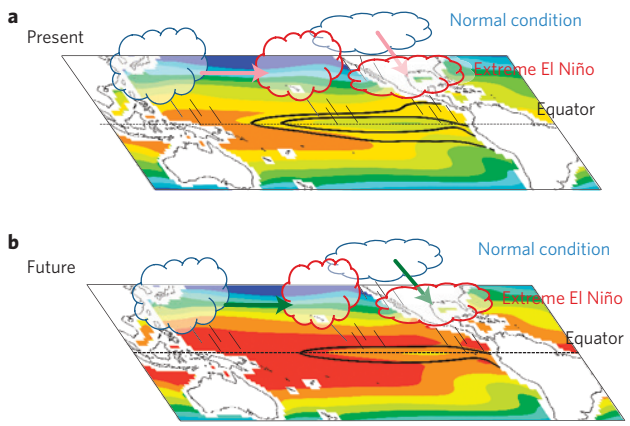

Figure 4 | Schematic depicting the mechanism for increased occurrences of extreme El Niño under greenhouse warming. a,**b**, In both present-day climate (**a**) and future climate (**b**), convection zones in the western Pacific and the ITCZ latitudes shift from their normal positions (indicated by blue clouds) to the eastern equatorial Pacific during an extreme El Niño event (indicated by red clouds). Colour shading indicates mean SSTs and black contours indicate SST anomalies. Under greenhouse-gas-induced warming conditions, warming occurs everywhere but at a faster rate in the eastern equatorial Pacific, diminishing the zonal and meridional SST gradients. Strong SST gradients are a barrier to a shift in convection zones. Therefore, in the future climate, shifts in convection zones can be facilitated by weaker changes in SST and thus SST gradients (indicated by one black contour and by green arrows), as compared with the present-day climate in which stronger changes are required (indicated by two black contours and red arrows).

leading to increased extreme El Niño occurrences (Fig. 3b) even though neither the average amplitude of El Niño-related SST anomalies nor the frequency of El Niño is substantially changed[19].

The increased extreme El Niño events do not simply result from an increasing climatological rainfall, but from enhanced probability of the establishment of atmospheric deep convection in the eastern equatorial Pacific through the change in background conditions: as the Equator warms more rapidly than the SSTs at the climatological position of the ITCZ, it takes a relatively weaker SST anomaly as compared with the control period to establish the warmest water over the equatorial eastern Pacific (Fig. 4). Detrended SST anomalies averaged over extreme El Niño events are indeed slightly smaller in the climate change period than those in the control period. There is virtually no change in occurrences concurrent with high SST anomalies (for example, $>2\,^{\circ}C$), and most of the increased occurrences of extreme El Niño are associated with smaller SST anomalies (Fig. 3c). The increased frequency of convection in the eastern equatorial Pacific is further highlighted by a 66% increase in the occurrences of detrended Niño3 rainfall anomalies greater than 2 mm per day, with a strong inter-model consensus (Fig. 3d and Supplementary Table 8 and Fig. 17). In contrast, there is no robust change following the commonly used definition based on similarly detrended, standardized Niño3 SST anomalies (Supplementary Table 9). The increased occurrences of atmospheric convection in the eastern equatorial Pacific depict stronger air–sea interactions, with a 25% increase in the sensitivity of detrended rainfall to positive SST anomalies (Supplementary Fig. 18). Despite these fundamental changes, the spatial pattern of the associated rainfall teleconnection remains overall similar to that in the control period (Supplementary Fig. 19), suggesting that, at a given location, past extreme El Niño impacts will repeat more frequently in the future as the planet warms.

In summary, our result of greenhouse-induced increased occurrence of extreme El Niño events is in stark contrast with previous findings of no consensus in El Niño change; our robust results arise from the use of process-based metrics, such as SST gradients and the impacts of reorganization of atmospheric convection, that isolate the mechanism of extreme El Niño events. With a projected large increase in extreme El Niño occurrences, we should expect more occurrences of devastating weather events, which will have pronounced implications for twenty-first century climate.

Full methods and any associated references are available in the Supplementary Information.

Methods

Diagnosis of extreme El Niño events. We use rainfall data in the satellite era (1979–present)[23], and SSTs from a global reanalysis[22]. DJF rainfall averaged over the Niño3 region (150° W–90° W, 5° S–5° N) and meridional SST gradient in the eastern Pacific (150° W–90° W), calculated as the difference between the average over the off-equatorial (5° N–10° N) and equatorial box (2.5° S–2.5° N) regions, are used as atmospheric and oceanic indices to characterize extreme El Niño events. Rainfall increases nonlinearly with Niño3 SST, or with the meridional gradient. The nonlinearity is measured by the skewness of Niño3 precipitation, which is 2.75 in observations. DJF Niño3 rainfall greater than 5 mm per day defines an extreme El Niño event.

Selection of models. DJF Niño3 rainfall greater than 5 mm per day and rainfall skewness greater than 1 are used as criteria for model selection from a total of 19 CMIP3 (ref. 10) and 21 CMIP5 (ref. 11) CGCMs. One experiment (the first simulation) from each model is used, covering the period 1891–2090 using historical anthropogenic and natural forcings to 2000 for CMIP3 and 2005 for CMIP5, and then a future emission scenario SRESA2 for CMIP3 and the RCP8.5 for CMIP5. In addition, 33 SST-bias-corrected PPE experiments, conducted with the HadCM3 CGCM forced with historical radiative perturbations and a 1% per year CO_2 increase[12] for the future climate change runs, each covering a 200-year period, are used. Only 9 CMIP3 and 11 CMIP5 CGCMs meet the criteria (Supplementary Tables 1 and 2), yielding a mean skewness close to the observed (Supplementary Tables 1 and 2). The skewness criterion filters out models with an overly wet or cold and dry model east equatorial Pacific (Supplementary Figs 10 and 11). These biases generally reduce the skewness, and are associated with SSTs well below or above the convective threshold range of 26–28 °C (ref. 29), leading to overly subdued or active Niño3 rainfall variability. Out of 33 PPE experiments, 25 meet the skewness criterion. We derive changes in the frequency of extreme El Niño events by comparing the first 100 years (control period) to the later (climate change period) years. We also test the sensitivity of our results to varying definitions (Supplementary Tables 3–6).

Contrasts between extreme El Niño and zonal SPCZ events. Neither zonal SPCZ nor extreme El Niño is a subset of the other (Supplementary Fig. 5a). This is because zonal SPCZ events are more closely associated with the south off-equatorial minus the equatorial meridional SST gradients over the central Pacific longitudes (Supplementary Fig. 5b), instead of the north off-equatorial minus the equatorial SST gradients over the eastern Pacific longitudes, which characterize extreme El Niño (Fig. 2c,d and Supplementary Fig. 5c). An aggregation over the 20 selected CGCMs (Supplementary Figs 6–13 and Tables 1–2) and over 200 years shows that about 40% of all zonal SPCZ events are independent from extreme El Niño events (green dots, Supplementary Fig. 5a and Table 10), analogous to the 1991/92 event, with generally lower Niño3 rainfall and larger north off-equatorial minus equatorial SST gradients in the eastern Pacific, in contrast to those during extreme El Niño events that can occur without zonal SPCZ events (about 20%, purple dots in Supplementary Fig. 5a). Supplementary Fig. 5b–e further contrasts the SST and rainfall anomaly patterns associated with independent zonal SPCZ events from those during extreme El Niño events in which the anomalies extend farther east into the Niño3 region.

Total rainfall change. The total rainfall change in the eastern equatorial Pacific under greenhouse warming ($\Delta Rain_{total}$) contains contributions from a change in the annual cycle ($\Delta Rain_{annual\text{-}cycle}$), a long-term trend ($\Delta Rain_{long\text{-}term}$), and a change in the response of rainfall to changing El Niño/Southern Oscillation (ENSO; $\Delta Rain_{ENSO}$). For a given season, the $\Delta Rain_{annual\text{-}cycle}$ and $\Delta Rain_{long\text{-}term}$ terms can be combined to a total long-term trend, $\Delta Rain_{total\text{-}long\text{-}term}$, such that

$$\Delta Rain_{total} = \Delta Rain_{total\text{-}long\text{-}term} + \Delta Rain_{ENSO}$$

As ENSO is seasonally phase-locked, peaking in austral summer, if there is a trend due to the response to ENSO, the total rainfall trend will include the contribution from $\Delta Rain_{ENSO}$, which would be at least partially removed by the detrending process. To understand how the distribution of rainfall anomalies will change, rainfall is quadratically detrended. The detrending process might partially remove the rainfall increase due to the increased frequency of extreme El Niño events.

Statistical significance test. We use a bootstrap method[27] to examine whether the change in frequency of the extreme El Niño events is statistically significant. The 2,000 DJF samples from the 20 selected CGCMs in the control period are re-sampled randomly with replacement to construct 10,000 realizations. The standard deviation of the extreme El Niño frequency in the inter-realization is 9.8 events per 2,000 years, far smaller than the difference between the control and the climate change periods at 111 events per 2,000 years (Fig. 2c,d), indicating statistical significance of the difference.

Received 15 October 2013; accepted 11 December 2013; published online 19 January 2014

References

1. Changnon, S. A. *El Niño, 1997–1998: The Climate Event of the Century* (Oxford Univ. Press, 2000).
2. McPhaden, M. J. El Niño: The child prodigy of 1997–98. *Nature* **398,** 559–562 (1999).
3. Philander, S. G. H. Anomalous El Niño of 1982–83. *Nature* **305,** 16 (1983).
4. Glynn, P. W. & de Weerdt, W. H. Elimination of two reef-building hydrocorals following the 1982–83 El Niño. *Science* **253,** 69–71 (1991).
5. Aronson, R. B. *et al.* Coral bleach-out in Belize. *Nature* **405,** 36 (2000).
6. Wilhite, D. A., Wood, D. A. & Meyer, S. J. in *Climate Crisis* (eds Glantz, M., Katz, R. & Krenz, M.) 75–78 (UNEP, 1987).
7. Vos, R., Velasco, M. & Edgar de Labastida, R. *Economic and social effects of El Niño in Ecuador, 1997–1998* (Inter-American Development Bank, Sustainable Development Dept. Technical papers series POV-107, 1999).
8. Vincent, E. M. *et al.* Interannual variability of the South Pacific Convergence Zone and implications for tropical cyclone genesis. *Clim. Dynam.* **36,** 1881–1896 (2011).
9. Cai, W. *et al.* More extreme swings of the South Pacific convergence zone due to greenhouse warming. *Nature* **488,** 365–369 (2012).
10. Meehl, G. *et al.* The WCRP CMIP3 multimodel dataset: A new era in climate change research. *Bull. Am. Meteorol. Soc.* **88,** 1383–1394 (2007).
11. Taylor, K. E., Stouffer, R. J. & Meehl, G. A. An overview of CMIP5 and the experimental design. *Bull. Am. Meteorol. Soc.* **93,** 485–498 (2012).
12. Collins, M. *et al.* A comparison of perturbed physics and multi-model ensembles: Model errors, feedbacks and forcings. *Clim. Dynam.* **36,** 1737–1766 (2011).
13. Xie, S. P. *et al.* Global warming pattern formation: Sea surface temperature and rainfall. *J. Clim.* **23,** 966–986 (2010).
14. Tokinaga, H., Xie, S-P., Deser, C., Kosaka, Y. & Okumura, Y. M. Slowdown of the Walker circulation driven by tropical Indo-Pacific warming. *Nature* **491,** 439–443 (2012).
15. Valle, C. A. *et al.* The Impact of the 1982–1983 E1 Niño-Southern Oscillation on Seabirds in the Galapagos Islands, Ecuador. *J. Geophys. Res.* **92,** 14437–14444 (1987).
16. Merlen, G. The 1982–1983 El Niño: Some of its consequences for Galapagos wildlife. *Oryx* **18,** 210–214 (1984).
17. Sponberg, K. *Compendium of Climatological Impacts, University Corporation for Atmospheric Research* Vol. 1 (National Oceanic and Atmospheric Administration, Office of Global Programs, 1999).
18. Timmermann, A. *et al.* Increased El Niño frequency in a climate model forced by future greenhouse warming. *Nature* **398,** 694–697 (1999).
19. Collins, M. *et al.* The impact of global warming on the tropical Pacific Ocean and El Niño. *Nature Geosci.* **3,** 391–397 (2010).
20. Yeh, S-W. *et al.* El Niño in a changing climate. *Nature* **461,** 511–514 (2009).
21. Kug, J-S., An, S. I., Ham, Y. G. & Kang, I-S. Changes in El Niño and La Niña teleconnection over North Pacific–America in the global warming simulations. *Theor. Appl. Climatol.* **100,** 275–282 (2010).
22. Rayner, N. A. *et al.* Global analyses of sea surface temperature, sea ice, and night marine air temperature since the late nineteenth century. *J. Geophys. Res.* **108,** 4407 (2003).
23. Adler, R. F. *et al.* The Version-2 Global Precipitation Climatology Project (GPCP) Monthly Precipitation Analysis (1979–present). *J. Hydrometeorol.* **4,** 1147–1167 (2003).
24. Ashok, K., Behera, S. K., Rao, S. A., Weng, H. & Yamagata, T. El Niño Modoki and its possible teleconnection. *J. Geophys. Res.* **112,** C11007 (2007).
25. Lengaigne, M. & Vecchi, G. A. Contrasting the termination of moderate and extreme El Niño events in coupled general circulation models. *Clim. Dynam.* **35,** 299–313 (2010).
26. Chiodi, A. M. & Harrison, D. E. Characterizing warm-ENSO variability in the equatorial Pacific: An OLR perspective. *J. Clim.* **23,** 2428–2439 (2010).
27. Austin, P. C. Bootstrap methods for developing predictive models. *Am. Stat.* **58,** 131–137 (2004).
28. Kim, D. *et al.* El Niño–Southern Oscillation sensitivity to cumulus entrainment in a coupled general circulation model. *J. Geophys. Res.* **116,** D22112 (2011).
29. Johnson, N. C. & Xie, S-P. Changes in the sea surface temperature threshold for tropical convection. *Nature Geosci.* **3,** 842–845 (2010).
30. Vecchi, G. A. & Soden, B. J. Global warming and the weakening of the tropical circulation. *J. Clim.* **20,** 4316–4340 (2007).

Acknowledgements

W.C., S.B. and P.v.R. are supported by the Australian Climate Change Science Program. W.C. is also supported by Goyder Research Institute, the CSIRO Office of Chief Executive Science Leader award, and Pacific Australia Climate Change Science Adaptation Programme. M.J.M. is supported by NOAA; PMEL contribution 4049. M.C. is supported by the NERC SAPRISE project (NE/I022841/1); A.T. is supported by NSF grant number 1049219; M.H.E. and A.S., by a grant under the ARC Laureate Fellowship scheme (FL100100214); L.W. by China National Natural Science Foundation Key Project(41130859); and E.G. by Agence Nationale pour la Recherche projects ANR-10-Blanc-616 METRO.

Author contributions

W.C. conceived the study in discussion with M.L. and G.V., and wrote the initial draft of the paper. S.B., P.v.R. and G.W. performed the analysis. M.C. conducted the perturbed physics ensemble climate change experiments with the HadCM3 model. All authors contributed to interpreting results, discussion of the associated dynamics, and improvement of this paper.

Additional information

Supplementary information is available in the online version of the paper. Reprints and permissions information is available online at www.nature.com/reprints. Correspondence and requests for materials should be addressed to W.C.

Competing financial interests

The authors declare no competing financial interests.